Submitted to Engineering Geology

Reliability Sensitivity Analysis of Geotechnical Monitoring Variables Using Bayesian Updating

Dian-Qing Li, State Key Laboratory of Water Resources and Hydropower Engineering Science, Institute of Engineering Risk and Disaster Prevention, Wuhan University; 8 Donghu South Road, Wuhan 430072, P. R. China. Email: dianqing@whu.edu.cn

Fu-Ping Zhang, State Key Laboratory of Water Resources and Hydropower Engineering Science, Institute of Engineering Risk and Disaster Prevention, Wuhan University; 8 Donghu South Road, Wuhan 430072, P. R. China. Email: fupingzhang@whu.edu.cn

Zi-Jun Cao, State Key Laboratory of Water Resources and Hydropower Engineering Science, Institute of Engineering Risk and Disaster Prevention, Wuhan University; 8 Donghu South Road, Wuhan 430072, P. R. China. Email: zijuncao@whu.edu.cn

Xiao-Song Tang, State Key Laboratory of Water Resources and Hydropower Engineering Science, Institute of Engineering Risk and Disaster Prevention, Wuhan University; 8 Donghu South Road, Wuhan 430072, P. R. China. Email: xstang@whu.edu.cn

Siu-Kui Au, Institute for Risk and Uncertainty, University of Liverpool; Harrison Hughes Building, Brownlow Hill, Liverpool, L69 3GH, United Kingdom. Email: siukuiau@liverpool.ac.uk

Corresponding author: **Zi-Jun Cao**

Tel: (86)-27-6877 4036

Fax: (86)-27-6877 4295

E-mail: zijuncao@whu.edu.cn

Abstract

Determining the sensitivity of monitoring variables is essential to field monitoring design for effectively monitoring the safety and reliability levels of geotechnical structures in uncertain environment. Reliability sensitivity analysis of monitoring variables provides a rational approach for identifying sensitive monitoring variables and is capable of accounting for geotechnical uncertainties. It, however, can be computationally expensive, especially when sophisticated numerical models (e.g., finite difference model, FDM) are involved and repeated simulation runs are required. This paper proposes a reliability sensitivity analysis method that leverages on the robustness of direct Monte Carlo simulation (MCS) and the Bayesian Updating with Structural Reliability Methods. The proposed approach allows performing the reliability sensitivity analysis of a monitoring variable by a single run of direct MCS, avoiding repeated simulation runs for different possible observational values of a given monitoring variable. Illustrative examples demonstrate the capability of the proposed approach in identifying the most sensitive monitoring variables among candidates. It is possible to achieve a significant reduction in the number of evaluations of numerical models for reliability sensitivity analysis of monitoring variables using the proposed approach.

Keywords: Monitoring design; Reliability analysis; Bayesian updating; Direct Monte Carlo simulation

1 Introduction

Geotechnical structures are frequently constructed and operated in highly uncertain environments due to the variability of load conditions and geo-materials that are affected by various geological processes and have undergone complex geological histories. For safety control and risk mitigation, field monitoring can be adopted in the field of engineering geology and geotechnical engineering to acquire information (e.g., displacement and groundwater level) reflecting safety and reliability levels of geotechnical structures by in-situ instrumentation (Juang et al., 2013; Schweckendiek and Vrouwenvelder, 2013; Peng et al., 2014; Yu et al., 2014; Kelly and Huang, 2015; Zhang et al., 2015; Camós et al., 2016; Ering and Babu, 2016; Li et al., 2016c, d; Hong et al., 2017; Xu et al., 2018; Zheng et al., 2018). Proper instrumentation is crucial to cost-effective field monitoring and rational assessment of geotechnical safety and reliability, which is usually accomplished through monitoring design. Monitoring design aims at identifying monitoring variables sensitive to the safety and reliability level of the subject geotechnical structure amidst various geotechnical uncertainties (such as those in soil/rock parameters and loads).

Reliability sensitivity analysis (Au, 2005; Sudret, 2008; Wang, 2012) provides a rigorous and rational framework for identifying sensitive monitoring variables from a pool of candidates (e.g., displacements at different locations of a slope). Under a reliability sensitivity analysis framework, the sensitivity of the reliability of a geotechnical system (e.g., slope) to a monitoring variable Z can be quantitatively reflected by the variation of failure probability, P_F, of the geotechnical system as a function of Z, which is referred to as the ‘failure probability

68 function' (FPF) with respect to the monitoring variable (i.e., FPFwMV) in this study.

69 Determining FPFwMV for the monitoring design, during which no monitoring
70 information has been obtained, requires one to calculate P_F for different prescribed values of
71 the monitoring variable concerned. This is a nontrivial task at least for two reasons. First, the
72 monitoring variable (e.g., displacements at some locations of a slope) may not be identical to
73 the design performance (e.g., safety factor of slope stability, *FS*) of geotechnical structures,
74 and they are usually linked through mathematical models, such as finite element model (FEM)
75 and finite difference model (FDM), in an implicit and indirect manner. For practical
76 applications, the model can be very complex and its evaluation is a computationally expensive
77 task. Second, incorporating the monitoring information into evaluation of P_F is frequently
78 performed under a Bayesian framework, in which the probability distribution of **x** is updated
79 based on monitoring information and P_F is re-evaluated using the updated probability
80 distribution (e.g., Hsiao et al., 2008; Straub, 2011; Papaioannou and Straub, 2012;
81 Schweckendiek and Vrouwenvelder, 2013; Wang et al., 2012; Zhang et al., 2013; Peng et al.,
82 2014; Li et al., 2016 b, c, d). By this means, determining FPFwMV often necessitates repeated
83 Bayesian analyses and reliability assessments of geotechnical structures for different values of
84 the monitoring variable concerned. This can be computationally prohibitive as complex models
85 are involved.

86 The above computational difficulty becomes more profound as the FPFwMV is evaluated
87 through simulation-based methods that are generally applicable to complex models, such as
88 Monte Carlo simulation (MCS) (e.g., Ang and Tang, 2007; Zhang et al., 2014, 2017; Li et al.,

89 2015; Gong et al., 2017, 2018; Xiao et al., 2018; Qi and Li, 2018), Markov Chain Monte Carlo
90 simulation (MCMCS) (e.g., Zhang et al., 2010, 2012; Wang and Cao, 2013; Cao and Wang,
91 2014), and Subset simulation (e.g., Au and Wang, 2014; Li et al., 2016a; Xiao et al., 2016;
92 Jiang et al., 2018). Previous studies (e.g., Au, 2005; Ching and Hsieh, 2007; Wang et al., 2010;
93 Wang, 2012; Yuan, 2013; Li et al., 2015) have developed several MCS-based methods for
94 efficient reliability sensitivity analyses. These methods provide the reliability sensitivity on
95 uncertain model parameters **x** (e.g., shear strength parameters) or design geometry parameters
96 (e.g., slope height and angle), which are directly used as input to evaluate the design
97 performance (e.g., *FS*) concerned. However, how to make use of MCS methods (e.g., direct
98 MCS) to efficiently evaluate the reliability sensitivity of geotechnical structures with respect
99 to monitoring variables, which are often implicit functions of **x**, remains an open question.

100 This paper develops a MCS-based method for reliability sensitivity analysis of monitoring
101 variables for geotechnical structures, which leverages on the robustness of direct Monte Carlo
102 simulation (MCS) and the recently established analogy between reliability and Bayesian
103 updating problem, i.e., the BUS (Bayesian Updating with Structural Reliability Methods)
104 framework (Straub and Papaioannou 2015). The proposed approach evaluates the FPFwMV
105 by a single run of direct MCS, avoiding repeated simulation runs for different possible
106 observational values of a given monitoring variable. This allows performing reliability
107 sensitivity analysis for identifying sensitive monitoring variables with complex computational
108 models, which accounts for various geological factors (e.g., geological discontinuities) in a
109 more detailed and realistic manner for the real world engineering problems, prior to the

monitoring. Moreover, if observational data are obtained during the monitoring, the updated reliability of geotechnical structure concerned can be directly read from the FPFwMV for real-time risk-based decision making, which is a nontrivial task because the posterior reliability analysis is often involved. The paper starts with the description of a general framework for reliability sensitivity analysis of monitoring variables, followed by development of the proposed approach. To improve the accuracy of the estimated FPFwMV, a modified rejection sampling principle is also developed. Finally, the proposed approach is illustrated using two geotechnical monitoring examples.

2 General framework for reliability sensitivity analysis of monitoring variables

Consider a geotechnical environment where one wants to determine a set of quantities for monitoring purpose. Fig.1 illustrates schematically the proposed reliability sensitivity analysis framework for monitoring variables. It starts with determining a number, M, of candidate monitoring variables Z_k (k = 1, 2, …, M) (e.g., displacements and groundwater level) based on site conditions and equipment availability. To effectively monitor the change in the reliability level of geotechnical structures (e.g., levee and slope), one needs to identify sensitive monitoring variables to guide in-situ instrumentation, which can be achieved by comparing the FPFs of candidate monitoring variables. For a given monitoring variable Z_k, the corresponding FPF is obtained by calculating failure probabilities $P_F(Z_k = z_{k,l})$ of the geotechnical structure at a number, N_k, of possible observational values (POVs), $z_{k,l}$, l = 1, 2, …, N_k, of Z_k. Herein, failure is defined in terms of the design performance (e.g., FS of slope stability) of the geotechnical

structure, which need not be the same as the monitoring variables. Note that, at the instrumentation design stage, monitoring information is not available, and some POVs of monitoring variables are prescribed for the reliability sensitivity analysis. For a given POV $z_{k,l}$ of Z_k, its corresponding P_F ($Z_k = z_{k,l}$) can be calculated through two steps: (1) determine the conditional probability distribution of uncertain model parameters $\mathbf{x}$, which are directly used to evaluate the geotechnical design performance, given $Z_k = z_{k,l}$; and (2) evaluate P_F ($Z_k = z_{k,l}$) based on the conditional probability distribution of $\mathbf{x}$, which are provided as below.

Using the Bayes' Theorem, the conditional probability density function (PDF) $f(\mathbf{x}|z_{k,l})$ of $\mathbf{x}$ given $Z_k = z_{k,l}$, often referred as the 'posterior PDF', can be expressed as:

$$f(\mathbf{x}|z_{k,l}) = f(z_{k,l}|\mathbf{x})f(\mathbf{x}) / f(z_{k,l}) \quad \text{for } k = 1, 2, \ldots, M \text{ and } l = 1, 2, \ldots, N_k \tag{1}$$

where $f(\mathbf{x})$ is the prior PDF of $\mathbf{x}$ and it reflects the knowledge on $\mathbf{x}$ in monitoring design stage where the monitoring information has not been obtained; $f(z_{k,l}|\mathbf{x})$ is the likelihood function that quantifies influence of $\mathbf{x}$ on Z_k; and $f(z_{k,l}) = \int f(z_{k,l}|\mathbf{x})f(\mathbf{x})d\mathbf{x}$ is the normalizing constant independent of $\mathbf{x}$. The formulation of the likelihood function is pivotal to evaluating the $f(\mathbf{x}|z_{k,l})$ in Eq. (1). It necessitates a mathematical model (e.g., FEM and FDM) to link $\mathbf{x}$ to Z_k. For a given mathematical model, the POV (i.e., $z_{k,l}$) of Z_k is modeled as:

$$z_{k,l} = M_k(\mathbf{x}) + \varepsilon_k \tag{2}$$

where $M_k(\mathbf{x})$ is the model prediction of the monitoring variable, referred as the monitoring performance function (MPF) of Z_k in this study; ε_k is assumed to be a Normal random variable with a mean value of μ_k and a standard deviation of σ_k, and it represents the model uncertainty associated with the mathematical model used to predict the value of Z_k. Using Eq. (2), the

likelihood function $f(z_{k,l}|\mathbf{x})$ is given by:

$$f\left(z_{k,l}\,|\,\mathbf{x}\right)=\frac{1}{\sqrt{2\pi}\sigma_k}\exp\left\{-\frac{[z_{k,l}-M_k(\mathbf{x})-\mu_k]^2}{2\sigma_k{}^2}\right\} \tag{3}$$

Based on Eq. (3) and prior PDF of $\mathbf{x}$, $f(\mathbf{x}|z_{k,l})$, is obtained using Eq. (1). Then, $P_F(Z_k= z_{k,l})$ is calculated as:

$$P_F(Z_k = z_{k,l})=P(F|Z_k = z_{k,l})=\int I\left[g(\mathbf{x})\le 0\right]f(\mathbf{x}|z_{k,l})d\mathbf{x} \tag{4}$$

where $g(\mathbf{x})$ is the design performance function (DPF) of a geotechnical structure (e.g., $g(\mathbf{x}) = FS$-1) and it is used to assess whether the performance (e.g., slope stability) of the geotechnical structure is satisfactory or not; and $I[\cdot]$ is an indicator function. $I[\cdot]$ is equal to 1 if the performance of the geotechnical structure is unsatisfactory, i.e., $g(\mathbf{x}) \le 0$, otherwise, it is equal to zero.

Note that the model uncertainties associated with the MPF and DPF affect the posterior distribution of uncertain model parameters (see Eqs. (1)-(3)) and posterior reliability analysis (see Eq. (4)), future studies on which are warranted. This is, however, out of the scope of this study. The values of model uncertainties in the illustrative examples later are simply adopted from those used in the literature to enable a consistent comparison with previous studies.

The calculation of $P_F(Z_k= z_{k,l})$ involves a number of evaluations of the MPF (for Bayesian analysis) and DPF (for the reliability analysis), which requires mathematical models to predict the monitoring variable and design performance given $\mathbf{x}$. Consider, for example, using direct MCS or MCMCS to evaluate $f(\mathbf{x}|z_{k,l})$ in Eq. (1) and to calculate $P_F\ (Z_k = z_{k,l})$ in Eq. (4) by generating N_{mcs} random samples of $\mathbf{x}$ (Beck and Au, 2002; Robert and Casella, 2004; Li et al., 2016c). This requires N_{mcs} evaluations of MPF and DPF (i.e., N_{mcs} evaluations of their

corresponding mathematical models), respectively. A direct way to obtain the FPF with respect to Z_k is repeatedly performing simulation runs at its N_k POVs to calculate their corresponding $P_F(Z_k = z_{k,l})$ values. By this means, $N_{mcs} \times N_k$ evaluations of MPF and DPF are needed. This is often computationally expensive, particularly for complex numerical models (e.g., FEM and FDM). The next section proposes an efficient method for evaluating FPFwMV, which only requires a single run of direct MCS.

3 Reliability sensitivity analysis of monitoring variables using direct MCS and BUS

3.1 Bayesian updating with structural reliability methods (BUS)

The proposed approach first evaluates the conditional PDF $f(\mathbf{x}|z_{k,l})$ given by Eq. (1) using a Bayesian updating technique recently developed by Straub and Papaioannou (2015), so-called Bayesian updating with structural reliability methods (BUS). BUS converts Bayesian updating problems into equivalent reliability analysis problems by constructing an observational failure domain (OFD) using the likelihood function. Reliability analysis methods (e.g., direct MCS) can then be used to evaluate the posterior distribution (e.g., Eq. (1)). In the context of BUS, the OFD in this study is defined as (Straub and Papaioannou, 2015; Cao et al., 2018):

$$\mathbf{\Omega}_{kl} = \left[\mathrm{U} \le c f(z_{k,l} \mid \mathbf{x}) \right] \tag{5}$$

where $\mathbf{\Omega}_{kl}$ represents the OFD for $Z_k = z_{k,l}$; c = a positive scalar constant ensuring $cf(z_{k,l}|\mathbf{x}) \le 1$ and it is taken as the reciprocal of the maximum value of the likelihood function $f(z_{k,l}|\mathbf{x})$ given by Eq. (3), i.e., $c = \sqrt{2\pi}\sigma_k$; and U = a uniform random variable ranging from zero to unity and it is independent of $\mathbf{x}$. Substituting Eq. (1) into Eq. (5) gives:

$$\boldsymbol{\Omega}_{kl} = \left[\mathrm{U} \le \frac{f(\mathbf{x}|z_{k,l})}{\left[cf(z_{k,l})\right]^{-1} f(\mathbf{x})} \right] \tag{6}$$

where $[cf(z_{k,l})]^{-1}$ is a constant independent of $\mathbf{x}$. The $f(\mathbf{x}|z_{k,l})$ and $f(\mathbf{x})$ in Eq. (6) can be, respectively, viewed as the target and sampling distributions according to rejection sampling principle (Au and Wang, 2014; Straub and Papaioannou, 2015; Cao et al., 2018). It is reasoned that random samples of $\mathbf{x}$ generated from $f(\mathbf{x})$ and satisfying $\boldsymbol{\Omega}_{kl}$ follow $f(\mathbf{x}|z_{k,l})$. In other words, the $\mathbf{x}$ samples distributed as $f(\mathbf{x}|z_{k,l})$ can be obtained by simulating conditional samples from $f(\mathbf{x})$ satisfying $\boldsymbol{\Omega}_{kl}$ defined by Eq. (5). For example, a direct MCS run is performed to generate N_{mcs} random samples of $\mathbf{x}$ from $f(\mathbf{x})$. The probability of each $\mathbf{x}$ sample falling into $\boldsymbol{\Omega}_{kl}$ is equal to $cf(z_{k,l}|\mathbf{x})$. The conditional samples of $\mathbf{x}$ satisfying $\boldsymbol{\Omega}_{kl}$ are selected from N_{mcs} unconditional samples by simulating N_{mcs} values, U_i, $i = 1, 2, \ldots, N_{mcs}$, of U and comparing the U_i value with $cf(z_{k,l}|\mathbf{x})$ for the i-th sample. If $\mathrm{U}_i \le cf(z_{k,l}|\mathbf{x}_i)$, the sample falls into $\boldsymbol{\Omega}_{kl}$ and is accepted as the conditional sample of $\mathbf{x}$ given $Z_k = z_{k,l}$; otherwise, it is rejected. By this means, a number, $N_{a,l}$, of $\mathbf{x}$ samples distributed as $f(\mathbf{x}|z_{k,l})$ are obtained, where $N_{a,l} < N_{mcs}$, and these samples are used to evaluate the FPF with respect to Z_k.

3.2 Calculating FPFwMV using direct MCS and BUS

The conditional samples (i.e., $\mathbf{x}_j, j = 1, 2, \ldots, N_{a,l}$) of $\mathbf{x}$ obtained from direct MCS and BUS represent $f(\mathbf{x}|z_{k,l})$ numerically, and they are used in Eq. (4) to evaluate $P_F(Z_k = z_{k,l})$:

$$P_F(Z_k = z_{k,l}) = \int I[g(\mathbf{x}) \le 0] f(\mathbf{x}|z_{k,l}) d\mathbf{x} = \frac{1}{N_{a,l}} \sum_{j=1}^{N_{a,l}} I[g(\mathbf{x}_j) \le 0] \tag{7}$$

A straightforward way to obtain FPF with respect to monitoring variable Z_k is to perform repeated runs of direct MCS and BUS for the N_k POVs (i.e., $z_{k,l}$, $l = 1, 2, \ldots, N_k$) of Z_k to obtain their corresponding failure probabilities. By this means, N_k direct MCS runs are needed, and the total computational efforts include $N_{mcs} \times N_k$ evaluations of the MPF in Bayesian analysis and $\sum_{l=1}^{N_k} N_{a,l}$ evaluations of the DPF, which remains a computationally expensive task.

Alternatively, this study proposes a sample-based strategy to select conditional samples of $\mathbf{x}$ given different POVs of Z_k based on the same set of unconditional samples generated from $f(\mathbf{x})$ using direct MCS, by which the FPF with respect to Z_k is evaluated by a single direct MCS run. Under the BUS framework, selection of the conditional samples of $\mathbf{x}$ from direct MCS samples depends on the likelihood function and the POV (i.e., $z_{k,l}$) of Z_k (see Eq.(5)). As $z_{k,l}$ changes from $z_{k,1}$ to $z_{k,Nk}$, the likelihood function changes, so does $\boldsymbol{\Omega}_{kl}$. On the contrary, direct MCS samples simulated from $f(\mathbf{x})$ are independent of $z_{k,l}$. Based on these observations, the respective conditional samples of $\mathbf{x}$ given different POVs of Z_k can be identified from the same set of direct MCS samples generated from $f(\mathbf{x})$ to calculate their corresponding failure probabilities without the need of performing repeated simulation runs for different POVs of Z_k. The implementation procedure is summarized in Fig. 2:

(1) Determine N_k POVs (i.e., $z_{k,l}$, $l = 1, 2, \ldots, N_k$) of Z_k for reliability sensitivity analysis;

(2) Generate N_{mcs} samples (i.e., $\mathbf{x}_1, \mathbf{x}_2, \ldots, \mathbf{x}_{Nmcs}$) of $\mathbf{x}$ from $f(\mathbf{x})$ by direct MCS;

(3) Calculate respective values of the likelihood function $f(z_{k,l}|\mathbf{x})$ (see Eq. (3)) for $z_{k,l}$ given $\mathbf{x}_1, \mathbf{x}_2, \ldots, \mathbf{x}_{Nmcs}$, and their corresponding acceptance probabilities $cf(z_{k,l}|\mathbf{x})$ as conditional samples of $\mathbf{x}$ given $Z_k = z_{k,l}$;

(4) Generate N_{mcs} random numbers (i.e., U_1, U_2, …, U_{Nmcs}) from a uniform distribution ranging from zero to unity, each of which corresponds to one **x** sample generated in step (2) and is used to determine whether the **x** sample satisfies Eq. (5) or not. This step selects $N_{a,l}$ conditional samples of **x** from N_{mcs} unconditional samples generated in step (3);

(5) Evaluate $P_F(Z_k = z_{k,l})$ by Eq. (7) based on the $N_{a,l}$ conditional samples of **x** obtained in step (4);

(6) Repeat steps (3)-(5) N_k times for $z_{k,l}$, $l = 1, 2, \ldots, N_k$, to obtain their corresponding values of $P_F(Z_k = z_{k,l})$.

The values of $P_F(Z_k = z_{k,l})$ obtained from the above procedure provide a discrete approximation of the FPF with respect to Z_k. During the calculation, direct MCS samples generated in step (2) remain unchanged. Hence, the MPF values (i.e., $M_k(\mathbf{x}_1)$, $M_k(\mathbf{x}_2)$, ..., $M_k(\mathbf{x}_{Nmcs})$) needed for evaluating the likelihood function in step (3) are the same for different POVs of Z_k. Only N_{mcs} evaluations of MPF are needed in Bayesian analyses with different POVs of Z_k, leading to significant reduction in computational efforts. Specifically, $N_{mcs} \times (N_k - 1)$ evaluations of MPF are avoided in comparison with using repeated simulation runs. For different POVs, their corresponding OFDs (i.e., Ω_{kl}, $l = 1, 2, \ldots, N_k$) may share some conditional samples because the OFDs of different POVs of Z_k may intersect and their conditional samples are selected from the same set of direct MCS samples. As a result, using the sample-based strategy proposed in this study, the number of evaluations of DPF needed in reliability analyses (i.e., step (5)) is less than $\sum_{l=1}^{N_k} N_{a,l}$. The computational effort for evaluating FPF with respect to Z_k is further reduced.

In the above procedure, determining conditional samples for different POVs of Z_k (see steps (2)-(4)) follows the original rejection sampling (ORS) principle (e.g., Au and Wang, 2014; Straub and Papaioannou, 2015), by which each unconditional sample of $\mathbf{x}$ has a probability of $cf(z_{k,l}|\mathbf{x})$ to be accepted as the conditional sample. The expected number $E(N_{a,l})$ of conditional samples given $Z_k = z_{k,l}$ is equal to $\sum_{i=1}^{N_{mcs}} cf(z_{k,l}|\mathbf{x}_i)$. However, due to random fluctuation in simulating $U_1, U_2, \ldots, U_{Nmcs}$ in step (4), the $N_{a,l}$ value determined from a given set of direct MCS samples can be either less or greater than $E(N_{a,l})$. This subsequently results in the fluctuation of estimated $P_F(Z_k = z_{k,l})$ in step (5) of the proposed sample-based strategy. More importantly, the number $N_{a,l}$ of conditional samples obtained in step (4) may not be sufficient to give an accurate estimate of $P_F(Z_k = z_{k,l})$ for different POVs. To address these issues, this paper proposes a modified rejection sampling (MRS) principle in the next section and combines the MRS principle with the sample-based strategy developed in this section to improve the accuracy of estimated $P_F(Z_k = z_{k,l})$.

4 Modified rejection sampling principle

As mentioned above, the unconditional sample generated by direct MCS is accepted or rejected as the conditional samples based on a probabilistic criterion (see Eq. (5)) according to the ORS principle. An unconditional sample $\mathbf{x}_i$ ($i = 1, 2, \ldots, N_{mcs}$) is accepted as the conditional sample if the random number U_i is less than the acceptance probability $cf(z_{k,l}|\mathbf{x}_i)$ of $\mathbf{x}_i$; otherwise, it is rejected. In other words, for a given POV (e.g., $z_{k,l}$) of Z_k, the acceptance or rejection of $\mathbf{x}_i$ as the conditional sample depends on the random sample U_i of U ranging zero and unity. Due to

the randomness in U, the $\mathbf{x}_i$ may or may not be the conditional sample in different simulation runs that generate different U values, resulting in random fluctuation of conditional samples of $\mathbf{x}$ determined using ORS based on the same set of unconditional samples.

With the understanding of the random mechanism of determining conditional samples by ORS, the MRS principle is proposed in this study, which consists of a number, N_r, of ORS runs based on the same set of direct MCS samples (e.g., $\mathbf{x}_1$, $\mathbf{x}_2$, ..., $\mathbf{x}_{Nmcs}$) to reduce the random fluctuation of conditional samples. As for the sample-based strategy described in the preceding subsection, this means repeatedly performing step (4) N_r times based on the same set of unconditional samples generated in step (2), as shown in Fig. 2 by dashed lines. Each run provides a set of conditional samples, which is denoted by $\mathbf{\Omega}_{kl,m}$, m = 1, 2, …, N_r. According to the ORS principle, the conditional samples in $\mathbf{\Omega}_{kl,m}$ follow the target PDF, e.g., posterior PDF $f(\mathbf{x}|z_{k,l})$ of $\mathbf{x}$ under the BUS framework. Hence, the conditional samples in $\mathbf{\Omega} = [\mathbf{\Omega}_{kl,1}, \mathbf{\Omega}_{kl,2}, \ldots, \mathbf{\Omega}_{kl,Nr}]$ obtained in the N_r runs of ORS (i.e., MRS) also follow the posterior PDF of $\mathbf{x}$. These conditional samples of $\mathbf{x}$ are subsequently used to evaluate $P_F(Z_k = z_{k,l})$ in step (5) of the proposed sample-based strategy and to obtain the FPF with respect to Z_k in step (6).

Using the MRS principle, the unconditional samples (e.g., $\mathbf{x}_1$, $\mathbf{x}_2$, ..., $\mathbf{x}_{Nmcs}$) generated from $f(\mathbf{x})$ using direct MCS represent the $f(\mathbf{x})$ numerically and remain unchanged in different runs of ORS for determining conditional samples. Each unconditional sample $\mathbf{x}_i$ is considered N_r times by generating N_r samples of U, during which its acceptance probability $cf(z_{k,l}|\mathbf{x}_i)$ is fixed for a given $Z_k = z_{k,l}$, and the expected times of $\mathbf{x}_i$ to be accepted as conditional samples is equal to $cf(z_{k,l}|\mathbf{x}_i) \times N_r$. As N_r increases, the frequency of $\mathbf{x}_i$ (i = 1, 2, …, N_{mcs}) among conditional samples

297 in **Ω** obtained from the MRS principle converges to $cf(z_{k,l}|\mathbf{x}_i)\times N_r$, indicating that the random
298 fluctuation in conditional samples of **x** obtained using MRS is minimal for large values of N_r.
299 Correspondingly, the number of conditional samples in **Ω** converges to $\sum_{i=1}^{N_{mcs}} cf(z_{k,l}\,|\,\mathbf{x}_i)N_r$,
300 which increases with the increase of N_r. Both the increase in the number of conditional samples
301 of **x** and the reduction in random fluctuation of the conditional samples contribute to
302 improvement of the accuracy of estimated $P_F(Z_k = z_{k,l})$. Such an improvement is at the expense
303 of ignorable additional computational costs in comparison of using ORS in the proposed
304 sample-based strategy because the unconditional samples (e.g., $\mathbf{x}_1$, $\mathbf{x}_2$, ..., $\mathbf{x}_{N_{mcs}}$) and their
305 corresponding likelihood functions $f(z_{k,l}|\mathbf{x}_i)$ for a given $Z_k = z_{k,l}$ are fixed in the N_r runs of ORS.
306 Determinating N_r is essential to the MRS principle. Since increasing N_r leads to ignorable
307 additional computational effort, a relatively large value (e.g., $N_r > 50$) of N_r is suggested. On
308 the other hand, as N_r increases, the frequency of $\mathbf{x}_i$ (i = 1, 2, …, N_{mcs}) among conditional
309 samples in **Ω** converge to $cf(z_{k,l}|\mathbf{x}_i)\times N_r$, leading to a stationary distribution of conditional
310 samples of **x**, and the convergence in estimated $P_F(Z_k = z_{k,l})$. In such case, it is not necessary to
311 further increase N_r. This study suggests determining the N_r adaptively based on the converge
312 check of estimated $P_F(Z_k = z_{k,l})$, which is demonstrated using the illustrative example in the
313 next section.
314

315 **5. Illustration and validation of FPFwMV using a levee head monitoring example**

316 With a complex numerical model (e.g., FDM and FEM), it is computationally prohibitive to
317 validate the FPFwMV obtained from the proposed approach. To illustrate and validate the

318 proposed approach for evaluating FPFwMV, this section uses a levee head monitoring example
319 with explicit MPF and DPF. The next section illustrates the application of the proposed
320 approach in the displacement monitoring design of a rock slope based on FDM.

321 The levee head monitoring example concerns about the occurrence of uplift on the
322 downstream side of the levee shown in Fig. 3. The example was used to illustrate reliability
323 updating with hydraulic head monitoring data under a Bayesian framework by Schweckendiek
324 and Vrouwenvelder (2013) and Schweckendiek (2014). As shown in Fig. 3, there is an aquifer
325 underlying the levee with a blanket layer on the downstream side with low permeability. The
326 hydraulic head ϕ_{exit} at the potential exit location in the aquifer just under the lower blanket
327 boundary is monitored in this example. The MPF is given by (Schweckendiek and
328 Vrouwenvelder 2013):

329 $$\phi_{exit}=h_p+\lambda(h-h_p)+\varepsilon \tag{8}$$

330 where h_p = phreatic surface in or above the blanket layer at the monitoring location, assumed
331 to be equal to water level h_s at the downstream surface; h = upperstream water level, taken to
332 be 3.9 m for a 100 year return period; λ = a damping factor for predicting the head difference
333 in the aquifer at the potential exit point; ε = a Normal variable with mean μ_ε=0 and standard
334 deviation σ_ε =0.1 m, modeling the error between the monitoring value and model prediction of
335 ϕ_{exit}, which are adopted from those used by Schweckendiek and Vrouwenvelder (2013) to
336 enable a consistent comparison. Uplift occurs as the hydraulic head difference $\Delta\phi$ between ϕ_{exit}
337 and h_p exceeds the hydraulic resistance that is represented by the critical uplift head difference
338 $\Delta\phi_c'$. The uplift DPF is given by (Schweckendiek and Vrouwenvelder 2013):

$$g_{DPF}(\mathbf{x}) = \Delta\phi_c' - \Delta\phi \tag{9}$$

where $\Delta\phi$ and $\Delta\phi_c'$ are, respectively, calculated as:

$$\Delta\phi = \phi_{exit} - h_p = \lambda\left(h - h_p\right) \tag{10}$$

$$\Delta\phi_c' = m_u d\left(\gamma_{sat}/\gamma_w - 1\right) \tag{11}$$

and m_u = a model factor quantifying the uncertainty associated with the estimated critical uplift head difference; d = the blanket layer thickness at the monitoring point; γ_{sat} and γ_w are the saturated volumetric weight of the blanket layer and the volumetric weight of water, respectively. Using Eqs. (9)-(11), the levee uplift reliability in this example depends on h, h_p, d, m_u, λ, and γ_{sat}. The distribution types and statistics of these uncertain parameters are summarized in Table 1. Assuming no correlation based on prior information, the prior distribution is the product of marginal distributions of uncertain model parameters (e.g., Cao et al., 2016).

5.1 Computation steps for evaluating FPF with respect to ϕ_{exit}

This section focuses on the validation of FPFwMV obtained from the proposed approach, where only one monitoring variable is considered, i.e., $Z = \phi_{exit}$. To evaluate the FPF of ϕ_{exit}, the six steps of the proposed approach described in Subsection 3.2 are implemented as follows:

(1) For determining the POVs of ϕ_{exit}, the statistical information of uncertain model parameters summarized in Table 1 is used to generate 1,000,000 unconditional samples of uncertain model parameters by direct MCS. These samples are used to predict ϕ_{exit}, yielding 1,000,000 estimates of ϕ_{exit}. Using these estimates, the mean value μ_ϕ and standard deviation

σ_ϕ of ϕ_{exit} are calculated as 3.18 m and 0.36 m, respectively. A series of POVs of ϕ_{exit} ranging from $\mu_\phi - 3\times\sigma_\phi$ (i.e., 2.1 m) to 3.9 m are considered, as shown in Table 2. The lower bound (i.e., 2.1 m) of the range of ϕ_{exit} is determined as its lowest conceivable value based on the three-sigma rule (e.g., Duncan, 2000), and its upper bound is considered not exceeding a 100-year upperstream water level h=3.9 m in this example. Correspondingly, the normalized POVs $(\phi_{exit}-\mu_\phi)/\sigma_\phi$ of ϕ_{exit} in this example vary from –3.0 to 2.0 with an increment of 0.5, which are summarized in Table 2. Note that although the POVs of ϕ_{exit} are determined through direct MCS in this example, this is not necessary for implementing the proposed approach because POVs of monitoring variables can also be determined or selected by engineering experience and judgments;

(2) If direct MCS is performed to determine POVs of ϕ_{exit} in step (1), the 1,000,000 unconditional samples generated in step (1) are used in this step; otherwise, a direct MCS run is performed to generate unconditional samples from the prior distribution;

(3) For each POV of ϕ_{exit} shown in Table 2, the respective values of likelihood function for different unconditional samples of uncertain model parameters generated in step (1) or (2) are calculated by:

$$f\left(\phi_{exit} \mid \mathbf{x}\right) = \frac{1}{\sqrt{2\pi}\sigma_\varepsilon} \exp\left\{-\frac{[\phi_{exit} - h_p - \lambda(h - h_p)]^2}{2\sigma_\varepsilon{}^2}\right\} \tag{12}$$

and the acceptance probability of unconditional samples is calculated as $cf(\phi_{exit}|\mathbf{x})$, where c is taken as equal to $\sqrt{2\pi}\sigma_\varepsilon \approx 0.25$ in this example;

(4) Generate 1,000,000 random numbers uniformly distributed from zero to unity, each of which corresponds to one unconditional sample generated in previous steps and is used to

381 determine whether the sample is accepted as a conditional sample according to its acceptance
382 probability calculated in step (3);
383 (5) By the MRS principle, step (4) is repeatedly performed N_r times to reduce the random
384 fluctuation in selected conditional samples, which are subsequently used to evaluate the
385 conditional uplift failure probability given a POV of ϕ_{exit}. Here, the N_r is gradually increased
386 until the estimated uplift failure probability converges. For example, Fig. 4 shows the variation
387 of the uplift failure probability $P_F(\phi_{exit}$=2.1 m) given ϕ_{exit} = 2.1 m with the increase of N_r. As
388 N_r increases from 1 to 20, the estimated $P_F(\phi_{exit}$=2.1 m) value gradually converges to 0.0020.
389 A relatively large value (i.e., 100) of N_r is adopted in the MRS principle to ensure the
390 convergence of the uplift failure probability;
391 (6) Repeat steps (3)-(5) for each POV of ϕ_{exit} shown in Table 2 to obtain their
392 corresponding conditional uplift failure probabilities, which provide a discrete approximation
393 of the FPF with respect to ϕ_{exit}.
394
395 ***5.2 FPF with respect to the hydraulic head at the monitoring location***
396 Fig. 5 shows the FPF with respect to ϕ_{exit} obtained from the proposed approach by a line with
397 circles. As the normalized POVs of ϕ_{exit} increases from −3 to 2 (i.e., ϕ_{exit} increases from 2.1 to
398 3.9 m), the uplift failure probability increases by two orders of magnitude from 0.0020 to 0.19.
399 Monitoring the hydraulic head effectively senses the variation of the occurrence plausibility of
400 uplift. Moreover, the FPF with respect to ϕ_{exit} provides an overview of the variation of the uplift
401 reliability as a function of ϕ_{exit} prior to monitoring instrumentation. Based on the FPF with

402 respect to ϕ_{exit}, the uplift failure probability can be determined directly from the observational
403 value of ϕ_{exit} during monitoring, which facilitates real-time risk-based decision making. For
404 example, as the observational value of ϕ_{exit} is equal to 2.3 m, the corresponding uplift failure
405 probability reads as around 0.0042 from the FPF shown in Fig. 5, which is consistent with the
406 value (0.0048) reported by Schweckendiek and Vrouwenvelder (2013).
407
408 ***5.3 Results comparison***
409 For further validation, the uplift failure probabilities given different POVs are also calculated
410 using a total of 11 runs of MCMCS. In each run, 1,000,000 MCMCS samples are generated to
411 numerically represent the posterior distribution given by Eq. (1) and to evaluate the uplift
412 failure probability given by Eq. (4) for a POV of ϕ_{exit}. Fig. 5 also includes the FPF with respect
413 to ϕ_{exit} obtained from repeated MCMCS runs by a line with squares. The lines with circles and
414 squares are close to each other. This indicates that the two sets of results obtained from the
415 proposed approach and repeated MCMCS runs are in a good agreement. This validates the
416 proposed approach. It is should be noted that only one direct MCS run is used to evaluate the
417 FPF with respect to ϕ_{exit} by the proposed approach, avoiding performing repeated simulation
418 runs for different POVs of ϕ_{exit}.
419 For a given POV of ϕ_{exit}, using the MRS principle in the proposed approach needs to re-
420 run N_r (e.g., 100) times of ORS for selection of conditional samples of uncertain model
421 parameters based on the same set of unconditional samples. The computational effort needed
422 in the proposed approach with MRS is, however, comparable with those needed for using the

423 proposed approach with ORS (i.e., $N_r = 1$) because the additional computational effort needed
424 for re-running ORS based on the same set of unconditional samples is negligible. For
425 comparison, Fig. 5 shows the FPF with respect to ϕ_{exit} obtained from the proposed approach
426 with ORS by a line with triangles. When the uplift failure probability is greater than 0.01, the
427 FPF obtained from the proposed approach with ORS agrees well with that obtained from the
428 proposed approach with MRS and repeated MCMCS runs. The agreement deteriorates as the
429 uplift failure probability is less than 0.01. The FPF obtained using ORS is not accurate at low
430 failure probability levels, while using the MRS in the proposed approach provides consistent
431 results.

432 Fig. 6 compares the coefficient of variation (COV) of the uplift failure probability at the
433 same POV of ϕ_{exit} obtained from the proposed approach with ORS and MRS (see triangles and
434 circles, respectively). The COV value at a given POV of ϕ_{exit} in Fig. 6 is calculated from 100
435 estimates of the uplift failure probability at the POV obtained from 100 runs of the proposed
436 approach with ORS or MRS. As shown in Fig. 6, for a given POV of ϕ_{exit}, the triangle always
437 appears above the circle. Using the MRS principle in the proposed approach leads to reduction
438 in COV of the estimated uplift failure probability. These observations demonstrate the benefit
439 of using the MRS principle in the proposed approach, particularly in relatively low failure
440 probability regime.

441

442 **6. Reliability sensitivity analysis for rock slope displacement monitoring using FDM**

443 The proposed approach with MRS is next applied to analyzing the reliability sensitivity on

surface displacements monitored at different locations of a rock slope example (Li et al., 2016c). As shown in Fig. 7, the rock slope has a height of 12 m and a slope angle of 60°. There is a joint extending from the slope toe to the height of 7.65 m in a direction at an angle of 35° to the horizontal. It intersects a vertical tension crack that locates behind the slope crest at a distance of 4 m and has a depth of 4.35 m. The groundwater condition is also shown in Fig. 7, and is characterized by the ratio r_w of water depth D_w over the crack depth D_c, i.e., $r_w = D_w / D_c$, which is represented by a truncated exponential variable ranging from 0 to 1 and having a mean of 0.1 (Li et al., 2016c). In addition to r_w, the cohesion c_J, friction angle ϕ_J, and Young's modulus E of the joint and the surcharge load p are represented by Normal random variables. Their statistics are summarized in Table 3, which are consistent with those adopted by Li et al. (2016c). In addition, as shown in Fig. 7, the slope is reinforced by four rows of rock bolts. For the sake of conciseness, more details on the rock bolts and the properties of rock masses are referred to Li et al. (2016c).

The *FS* of rock slope stability and the surface displacements are evaluated using FDM through a commercial software FLAC 7.0 (Itasca, 2014). Fig. 8 shows dimensions of the FDM that is discretized into 782 elements. The rock mass and the joint are modeled as elastic-perfectly plastic materials based on the Mohr-Coulomb strength criterion, and the rock bolts are modeled through cable elements. The bottom boundary is fixed in both horizontal and vertical directions and the right vertical boundary is constrained in horizontal direction. Moreover, the groundwater condition is considered through a groundwater table. The set-up of the FDM in this study is generally consistent with that adopted by Li et al. (2016c), which

465 provides more details on development of the FDM of the rock slope for interested readers.

466 For validation, the *FS* and surface displacements at two different points (i.e., A and B
467 shown in Fig. 7) are calculated using the FDM developed in this study under different surcharge
468 loads and groundwater levels, and the results are compared with those (including *FS*, vertical
469 displacement (V_A) at point A, and horizontal displacement (H_B) at point B) reported by Li et al.
470 (2016c). Fig. 9(a) shows the *FS*, V_A, and H_B calculated under different surcharge loads in this
471 study and Li et al. (2016c) by solid and dashed lines, respectively. The results obtained from
472 this study are consistent with those reported by Li et al. (2016c). Similar observations can also
473 be obtained from the *FS*, V_A, and H_B calculated under different groundwater levels, as shown
474 in Fig. 9 (b). This validates the FDM developed in this study. The FDM is subsequently used
475 in the proposed approach to evaluate FPF with respect to surface displacements for reliability
476 sensitivity analysis. This is different from Li et al. (2016c), where surrogate models (i.e.,
477 second-order polynomial response surfaces) are used to back analyze model parameters (e.g.,
478 r_w, c_J, ϕ_J, E, and p) for assessing slope stability safety and reliability based on monitoring
479 information under a Bayesian framework. The surrogate model is adopted to reduce
480 computational efforts needed in the back analysis, safety assessment, and reliability analysis
481 so that repeated simulation runs for different values of monitoring variables are tractable.
482 However, it shall be noted that the accuracy of surrogate model is problem-dependent. Future
483 studies on surrogate model-based Bayesian analyses, where the probability space of uncertain
484 parameters is updated with acquired information, are warranted, which is out of scope of this
485 study. Alternatively, this study tackles the computational difficulty arising from sophisticated

numerical models in evaluating FPFwMV through developing an efficient reliability sensitivity analysis method, where repeated simulation runs are avoided, as illustrated below.

6.1 Computation steps for evaluating FPFwMV in the rock slope example

For the purpose of reliability sensitivity analysis of monitoring variables, two additional monitoring locations (i.e., points C and D shown in Fig. 7) are considered besides points A and B in this study, whose horizontal and vertical displacements are also taken as monitoring variables. As a result, there are a total of eight monitoring variables Z_k, k = 1, 2, …, 8 (i.e., horizontal displacements H_A, H_B, H_C, and H_D, and vertical displacements V_A, V_B, V_C, and V_D), of points A to D. Then, the proposed approach with the MRS principle is applied to evaluating the FPF of each monitoring variable concerned (i.e., H_A, H_B, H_C, H_D, V_A, V_B, V_C, and V_D), which is described as follows:

(1) The implementation starts with prescribing POVs of monitoring variables. In this example, 13 POVs varying from 1 to 13mm at an interval of 1mm are considered for each monitoring variable;

(2) A direct MCS with 15,000 samples is simulated from the prior distribution of uncertain model parameters (i.e., r_w, c_J, ϕ_J, E, and p). Herein, assuming no correlation among uncertain model parameters based on prior information, the prior distribution is the product of their marginal distributions summarized in Table 3. Using 15,000 samples to evaluate the failure probability of the rock slope stability based on the prior distribution and FDM, where the model error in FS calculated by FDM is considered as a Normal distribution with a mean of 0 and standard deviation of 0.05 (Li et al. 2016c). The resulting failure probability is 25.5%,

508 which agrees well with the value (i.e., 24.9%) reported by Li et al. (2016c). This further
509 validates the uncertainty model and FDM developed in this study;

510 (3) For a given POV of the monitoring variable concerned, the values of the likelihood
511 function for the 15,000 unconditional samples are calculated using Eq. (3), where the MPF is
512 calculated using the FDM, and the acceptance probability of a given sample is evaluated as the
513 product of the constant $\sqrt{2\pi}\sigma_k$ and the likelihood function for the sample. In this example,
514 the prediction model error ε_k in surface displacements is represented by a Normal random
515 variable with a mean of 0 and standard deviation (i.e., σ_k) of 1 mm, which follow those
516 adopted by Li et al. (2016c);

517 (4) Generate 15,000 random numbers uniformly distributed from zero to unity, each of
518 which corresponds to one unconditional sample for selecting conditional samples;

519 (5) Step (4) is repeatedly performed 100 times (i.e., N_r = 100) to reduce the random
520 fluctuation in conditional samples, which are subsequently used to evaluate the conditional
521 failure probability of the rock slope stability given the POV of the monitoring variable
522 concerned by Eq. (7);

523 (6) Repeat steps (3)-(5) for each POV of the monitoring variable concerned to obtain
524 their corresponding conditional failure probabilities of the rock slope stability, which provide
525 a discrete approximation of the FPF of the monitoring variable.

526

527 ***6.2 FPFs with respect to surface displacements***

528 Fig. 10 shows the FPFs with respect to horizontal displacements (i.e., H_A, H_B, H_C, and H_D) and
529 vertical displacements (i.e., V_A, V_B, V_C, and V_D) by solid and dashed lines, respectively. As the

surface displacement increases, the slope failure probability increases by two to three orders of magnitude. This means that the reliability level of the rock slope stability is generally sensitive to surface displacements, particularly as the surface displacement is relatively small (say less than 7 mm in this example). It is also observed that the reliability sensitivity of the rock slope stability depends on the monitoring location because different FPFs are obtained for surface displacements at different locations. Comparing FPFs with respect to the eight monitoring variables reveals that the horizontal displacement H_B at point B (i.e., the slope toe) is the most sensitive monitoring variable while its vertical displacement V_B is the least sensitive one. It shall be emphasized that calculations of the FPFs of the eight monitoring variables are based on the same set of unconditional samples using the proposed approach. This avoids repeatedly performing direct MCS runs for different monitoring variables and for different POVs of a given monitoring variable in this example. The number of evaluations of numerical models needed for evaluating the FPFs is reduced considerably, leading to significant computational saving.

6.3 Reliability sensitivity to surface displacements at different locations

For detailed examination of the reliability sensitivity on different monitoring variables, a reliability sensitivity index (RSI) is defined in this example, and it is written as:

$$RSI_k = \frac{\ln P_F(Z_k = POV_{k,\max}) - \ln P_F(Z_k = POV_{k,\min})}{POV_{k,\max} - POV_{k,\min}} \tag{13}$$

where Z_k, k = 1, 2, …, 8, are the eight monitoring variables; $POV_{k,\,\min}$ and $POV_{k,\,\max}$ are the minimum and maximum POVs of Z_k, and they are, respectively, taken as 1 mm and 13 mm in

551 this example; $\ln P_F(Z_k = POV_{k,\min})$ and $\ln P_F(Z_k = POV_{k,\max})$ are logarithms of the conditional
552 failure probability of the rock slope stability given $Z_k = POV_{k,\min}$ and $POV_{k,\max}$, respectively.
553 The RSI_k represents the increasing rate of the rock slope failure probability as the surface
554 displacement increases from $POV_{k,\min}$ to $POV_{k,\max}$, and reflects the reliability sensitivity of the
555 rock slope stability with respect to Z_k ranging from $POV_{k,\min}$ to $POV_{k,\max}$. It provides a measure
556 to, quantitatively, compare the reliability sensitivity on different monitoring variables. The
557 greater the RSI_k is, the more sensitive to the reliability of the rock slope stability is. Table 4
558 summarizes the RSI_k values of the eight monitoring variables. The H_B has the maximum RSI
559 value (i.e., 0.58) among the eight monitoring variables while V_B has the minimum RSI value
560 (i.e., 0.36), which indicates that H_B and V_B are the most and least sensitive monitoring variables,
561 respectively. This is consistent with the observation obtained from the FPFs shown in Fig. 10.
562 Moreover, as shown in Table 4, the reliability sensitivity of the rock slope stability to horizontal
563 displacements (i.e., H_A, H_C, H_D, and H_B) increases with the decrease of the elevation from point
564 A to point B. In contrast, the reliability sensitivity of the rock slope stability to vertical
565 displacements (i.e., V_A, V_C, V_D, and V_B) decreases with the decrease of the elevation from point
566 A to point B. This suggests that the instrumentation shall be installed to monitor the horizontal
567 displacement (i.e., H_B) at slope toe and the vertical displacement (i.e., V_A) at the top of tension
568 crack with the first priority.
569

570 **7 Summary and conclusions**

571 This paper proposed a reliability sensitivity analysis method that leverages on the robustness

572 of direct Monte Carlo simulation (MCS) and the recently established analogy between
573 reliability and Bayesian updating problem, i.e., the BUS (Bayesian Updating with Structural
574 Reliability Methods) framework. It allows one to use a single run of direct MCS to obtain
575 failure probability functions (FPF) with respect to different monitoring variables (FPFwMV)
576 for determining the most sensitive monitoring variables during monitoring design, where no
577 monitoring information is available. To reduce the random fluctuation of conditional samples
578 obtained from BUS, this study proposed a modified rejection sampling (MRS) principle that
579 consists of multiple runs of the original rejection sampling (ORS) based on the same set of
580 direct MCS samples.

581 The proposed approach has been illustrated and validated using a levee head monitoring
582 example with a single monitoring variable and explicit performance functions and a rock slope
583 example with multiple monitoring variables and implicit performance functions evaluated
584 through the finite difference model (FDM). Results showed that the proposed approach
585 efficiently generates the FPFwMV for monitoring design in the sense that it only needs a single
586 run of direct MCS and avoids repeated simulation runs for evaluating failure probability at
587 different possible observational values of a given monitoring variable. This leads to significant
588 reduction in computation efforts for reliability sensitivity analysis of monitoring variables,
589 particularly when sophisticated numerical models (e.g., FDM) is involved. Using the MRS
590 principle improves the accuracy of FPFs at the expense of ignorable additional computational
591 efforts in comparison with using ORS. In the rock slope example, the reliability sensitivity of
592 slope stability to vertical and horizontal surface displacements has opposite trends. As the

593 elevation of the monitoring location increases, the sensitivity to the horizontal displacement
594 decreases, but the sensitivity to the vertical displacement increases. As a result, the horizontal
595 displacement at the slope toe and the vertical displacement at the top of slope are the most
596 critical monitoring variables, where monitoring instruments shall be installed with the first
597 priority.

598 With the FPFwMV obtained prior to monitoring, in-situ instrumentation can be arranged
599 in a cost-effective manner, and determining the real-time reliability level of geotechnical
600 structures during monitoring is a trivial task. This is of great significance to practical
601 monitoring problems in real word, where complex numerical models are often involved for
602 detailed and realistic modeling of geotechnical structures concerned.

603

Acknowledgements

This work was supported by the National Key R&D Program of China (Project No. 2016YFC0800200), and the National Natural Science Foundation of China (Project Nos. 51579190, 51528901, 51679174). The second author would like to thank for the support of China Scholarship Council (No. 201606270085). The authors also would like to thank Dr. Xueyou Li for his advices on the calculation model of the rock slope example.

Reference

[1] Ang, A.H.S., Tang, W.H. (2007). Probability Concepts in Engineering: Emphasis on Applications to Civil and Environmental Engineering, seconded. John Wiley & Sons.

[2] Au, S.K. (2005). Reliability-based design sensitivity by efficient simulation. Computers and structures, 83(14):1048-61.

[3] Au, S.K., Wang, Y. (2014). Engineering risk assessment with subset simulation. John Wiley & Sons.

[4] Beck, J.L., Au, S.K. (2002). Bayesian updating of structural models and reliability using Markov chain Monte Carlo simulation. Journal of engineering mechanics, 128(4): 380-391.

[5] Cao, Z.J., Wang, Y. (2014). Bayesian model comparison and characterization of undrained shear strength. Journal of Geotechnical and Geoenvironmental Engineering, 140(6): 04014018.

[6] Cao, Z.J., Wang, Y., Li, D.Q. (2016). Quantification of prior knowledge in geotechnical site characterization. Engineering Geology, 203: 107-116.

[7] Cao, Z.J., Zheng, S., Li, D.Q., Phoon, K.K. (2018). Bayesian identification of soil stratigraphy based on soil behaviour type index. Canadian Geotechnical Journal, doi.org/10.1139/cgj-2017-0714.

[8] Camós, C., Špačková, O., Straub, D., Molins, C. (2016). Probabilistic approach to assessing and monitoring settlements caused by tunneling. Tunnelling and Underground Space Technology, 51: 313-325.

[9] Ching, J., Hsieh, Y.H. (2007). Local estimation of failure probability function and its confidence interval with maximum entropy principle. Probabilistic Engineering Mechanics, 22(1): 39-49.

[10] Duncan, J.M. (2000). Factors of safety and reliability in geotechnical engineering. Journal of geotechnical and geoenvironmental engineering, 126(4): 307-316.

[11] Ering, P., Babu, G.L.S. (2016). Probabilistic back analysis of rainfall induced landslide—a case study of Malin landslide, India. Engineering Geology, 208: 154-164.

[12] Gong, W., Juang, C.H., and Martin, J.R. (2017). A new framework for probabilistic analysis of the performance of a supported excavation in clay considering spatial variability. Géotechnique, 67(6): 546-552.

[13] Gong, W., Juang, C.H., Ii, J.R.M., Tang, H., Wang, Q., Huang, H. (2018). Probabilistic analysis of tunnel longitudinal performance based upon conditional random field simulation of soil properties. Tunnelling and Underground Space Technology, 73: 1-14.

[14] Hong, Y., Wang, L.Z., Ng, C. W.W., Yang, B. (2017). Effect of initial pore pressure on undrained shear behaviour of fine-grained gassy soil. Canadian Geotechnical Journal, 54(11): 1592-1600.

[15] Hsiao, E.C., Schuster, M., Juang, C.H., Kung, G.T. (2008). Reliability analysis and updating of excavation-induced ground settlement for building serviceability assessment. Journal of Geotechnical and Geoenvironmental Engineering, 134(10): 1448-1458.

[16] Itasca Consulting Group, Inc. 2014. https://www.itascacg.com/.

[17] Jiang, S.H., Papaioannou, I., Straub, D. (2018). Bayesian updating of slope reliability in spatially variable soils with in-situ measurements. Engineering Geology, 239: 310-320.

[18] Juang, C.H., Luo, Z., Atamturktur, S., Huang, H. (2013). Bayesian updating of soil parameters for braced excavations using field observations. Journal of Geotechnical and Geoenvironmental Engineering, 139(3): 395-406.

[19] Kyowa (2017). http://www.kyowa-ei.com/eng/product/sector/building/application_080.htm.

[20] Kelly, R., Huang, J. (2015). Bayesian updating for one-dimensional consolidation measurements. Canadian Geotechnical Journal, 52(9): 1318-1330.

[21] Li, D.Q., Zhang, F.P., Cao, Z.J., Zhou, W., Phoon, K.K., Zhou, C.B. (2015). Efficient reliability updating of slope stability by reweighting failure samples generated by Monte Carlo simulation. Computers and Geotechnics, 69: 588-600.

664 [22] Li, D.Q., Xiao, T., Cao, Z.J., Zhou, C.B., Zhang, L.M. (2016a). Enhancement of random
665 finite element method in reliability analysis and risk assessment of soil slopes using Subset
666 Simulation. Landslides, 13(2): 293-303.
667 [23] Li, S., Zhao, H., Ru, Z., Sun, Q. (2016b). Probabilistic back analysis based on Bayesian
668 and multi-output support vector machine for a high cut rock slope. Engineering Geology,
669 203: 178-190.
670 [24] Li, X.Y., Zhang, L.M., Jiang, S.H., Li, D.Q., Zhou, C.B. (2016c). Assessment of slope
671 stability in the monitoring parameter space. Journal of Geotechnical and
672 Geoenvironmental Engineering, 142(7): 04016029.
673 [25] Li, X.Y., Zhang, L.M., Jiang, S.H. (2016d). Updating performance of high rock slopes by
674 combining incremental time-series monitoring data and three-dimensional numerical
675 analysis. International Journal of Rock Mechanics and Mining Sciences, 83: 252-261.
676 [26] Papaioannou, I., Straub, D. (2012). Reliability updating in geotechnical engineering
677 including spatial variability of soil. Computers and Geotechnics, 42: 44-51.
678 [27] Peng, M., Li, X.Y., Li, D.Q., Jiang, S.H., Zhang, L.M. (2014) Slope safety evaluation by
679 integrating multi-source monitoring information. Structural safety, 49: 65-74.
680 [28] Qi, X.H. and Li, D.Q. (2018). Effect of spatial variability of shear strength parameters on
681 critical slip surfaces of slope. Engineering Geology, 239: 41-49.
682 [29] Schweckendiek, T., Vrouwenvelder, A. (2013). Reliability updating and decision analysis
683 for head monitoring of levees. Georisk: Assessment and Management of Risk for
684 Engineered Systems and Geohazards, 7(2): 110-121.

685 [30] Schweckendiek, T. (2014). On reducing piping uncertainties: A Bayesian decision
686 approach. TU Delft, Delft University of Technology.
687 [31] Sudret, B. (2008). Global sensitivity analysis using polynomial chaos expansions.
688 Reliability Engineering and System Safety, 93(7): 964-979.
689 [32] Straub, D. (2011). Reliability updating with equality information. Probabilistic
690 Engineering Mechanics, 26(2): 254-258.
691 [33] Straub, D., Papaioannou, I. (2015) Bayesian updating with structural reliability methods.
692 Journal of Engineering Mechanics, 141(3): 04014134.
693 [34] Wang, L., Ravichandran, N., Juang, C. H. (2012). Bayesian updating of KJHH model for
694 prediction of maximum ground settlement in braced excavations using centrifuge data.
695 Computers and Geotechnics, 44: 1-8.
696 [35] Wang, Y., Cao, Z.J., Au, S.K. (2010). Efficient Monte Carlo simulation of parameter
697 sensitivity in probabilistic slope stability analysis. Computers and Geotechnics, 37(7-8):
698 1015-1022.
699 [36] Wang, Y. (2012). Uncertain parameter sensitivity in Monte Carlo simulation by sample
700 reassembling. Computers and Geotechnics, 46: 39-47.
701 [37] Wang, Y., Cao, Z.J. (2013). Probabilistic characterization of Young's modulus of soil using
702 equivalent samples. Engineering Geology, 159: 106-118.
703 [38] Xiao, T., Li, D.Q., Cao, Z.J., Au, S.K., Phoon, K.K. (2016). Three-dimensional slope
704 reliability and risk assessment using auxiliary random finite element method. Computers
705 and Geotechnics, 79: 146-158.

706 [39] Xiao, T., Li, D.Q., Cao, Z.J., Zhang, L.M. (2018). CPT-based probabilistic
707 characterization of three-dimensional spatial variability using MLE. Journal of
708 Geotechnical and Geoenvironmental Engineering, 144(5): 04018023
709 [40] Xu, L., Coop, M. C., Zhang, M. S., Wang, G. L. (2018). The mechanics of a saturated silty
710 loess and implications for landslides. Engineering Geology, 236: 29-42.
711 [41] Yu, Y., Wang, E., Zhong, J., Liu, X., Li, P., Shi, M., Zhang, Z. (2014). Stability analysis
712 of abutment slopes based on long-term monitoring and numerical simulation. Engineering
713 Geology, 183: 159-169.
714 [42] Yuan, X. (2013). Local estimation of failure probability function by weighted approach.
715 Probabilistic Engineering Mechanics, 34: 1-11.
716 [43] Zhang, J., Huang, H.W., Zhang, L.M., Zhu, H.H., Shi, B. (2014). Probabilistic prediction
717 of rainfall-induced slope failure using a mechanics-based model. Engineering Geology,
718 168(1): 129-140.
719 [44] Zhang, J., Tang, W.H., Zhang, L.M., Huang, H.W. (2012). Characterising geotechnical
720 model uncertainty by hybrid Markov Chain Monte Carlo simulation. Computers and
721 Geotechnics, 43: 26-36.
722 [45] Zhang, J., Wang, H., Huang, H.W., Chen, L.H. (2017). System reliability analysis of soil
723 slopes stabilized with piles. Engineering Geology, 229(7): 45-52.
724 [46] Zhang, L.L., Zhang, J., Zhang, L.M., Tang, W.H. (2010). Back analysis of slope failure
725 with Markov chain Monte Carlo simulation. Computers and Geotechnics, 37(7): 905-912.

726 [47] Zhang, L.L., Zuo, Z.B., Ye, G.L., Jeng, D.S., Wang, J.H. (2013). Probabilistic parameter
727 estimation and predictive uncertainty based on field measurements for unsaturated soil
728 slope. Computers and Geotechnics, 48: 72-81.
729 [48] Zhang, W.G., Goh, A.T.C., Xuan, F. (2015). A simple prediction model for wall deflection
730 caused by braced excavation in clays. Computers and Geotechnics, 63: 67-72.
731 [49] Zheng, D., Huang, J., Li, D.Q., Kelly, R., Sloan, S.W. (2018). Embankment prediction
732 using testing data and monitored behaviour: A Bayesian updating approach. Computers
733 and Geotechnics, 93: 150-162.

Captions of Tables

Table 1. Summary of distribution types and statistics of uncertain model parameters in the levee monitoring example (after Schweckendiek and Vrouwenvelder 2013)

Table 2. Summary of possible observational values of the hydraulic head in the aquifer

Table 3. Prior distribution of uncertain model parameters of the rock slope example (after Li et al. 2016c)

Table 4. Reliability sensitivity index of different monitoring variables

Table 1. Summary of distribution types and statistics of uncertain model parameters in the levee monitoring example (after Schweckendiek and Vrouwenvelder 2013)

Model parameters	Distribution type	Statistical parameters	
		Mean	Standard deviation
Water lever h (m)	Gumbel	2.67	0.38
Surface level at the potential exit point h_p (m)	Normal	0.3	0.1
Blanket layer thickness d (m)	Lognormal	3.0	0.5
Model factor m_u	Lognormal	1.0	0.1
Saturated volumetric weight of the blanket layer γ_{sat} (kN/m^3)	Normal	20.0	1.0
Damping factor λ	Lognormal	0.8	0.1

Table 2. Summary of possible observational values of the hydraulic head in the aquifer

Possible observational value ϕ_{exit} (m)	2.10	2.28	2.46	2.64	2.82	3.00	3.18	3.36	3.54	3.72	3.90
Normalized value $(\phi_{exit} - \mu_\phi)/\sigma_\phi$	-3.0	-2.5	-2.0	-1.5	-1.0	-0.5	0	0.5	1.0	1.5	2.0

Table 3. Prior distribution of uncertain model parameters of the rock slope example (after Li et al. 2016c)

Parameter	Distribution type	Mean value	Coefficient of variation
Young's modulus E (MPa)	Normal	50	0.2
Cohesion c_J (kPa)	Normal	20	0.3
Friction angle ϕ_J (°)	Normal	32	0.2
Surcharge load p (kPa)	Normal	200	0.1
Groundwater level ratio r_w	Truncated exponential	0.1	1

Table 4. Reliability sensitivity index of different monitoring variables

Monitoring location	Monitoring variable	RSI_k	Rank
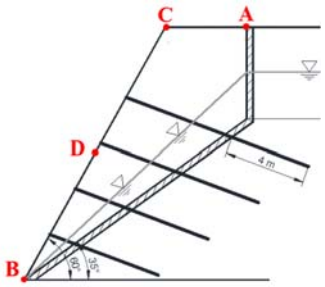	Z_1: H_A	0.40	7
	Z_2: H_B	0.58	1
	Z_3: H_C	0.42	6
	Z_4: H_D	0.51	3
	Z_5: V_A	0.55	2
	Z_6: V_B	0.36	8
	Z_7: V_C	0.47	4
	Z_8: V_D	0.43	5

Captions of Figures

Fig. 1. Reliability sensitivity analysis framework for monitoring variables

Fig. 2. Implementation procedure of the proposed sample-based strategy for evaluating FPFwMV

Fig. 3. The levee head monitoring example (after Schweckendiek and Vrouwenvelder 2013)

Fig. 4. Variation of the uplift failure probability given ϕ_{exit} = 2.1 m with the increase of N_r

Fig. 5. Comparison of uplift failure probability functions obtained by different methods

Fig. 6. Coefficients of variation of uplift failure probabilities calculated by the proposed approach with ORS and MRS

Fig. 7. Illustration of the rock slope example (after Li et al. 2016)

Fig. 8. The finite difference model for the rock slope example in FLAC 7.0

Fig. 9. Factor of safety and surface displacements at points A and B under different surcharge load and groundwater levels

Fig. 10. Failure probability functions with respect to different monitoring variables in the rock slope example

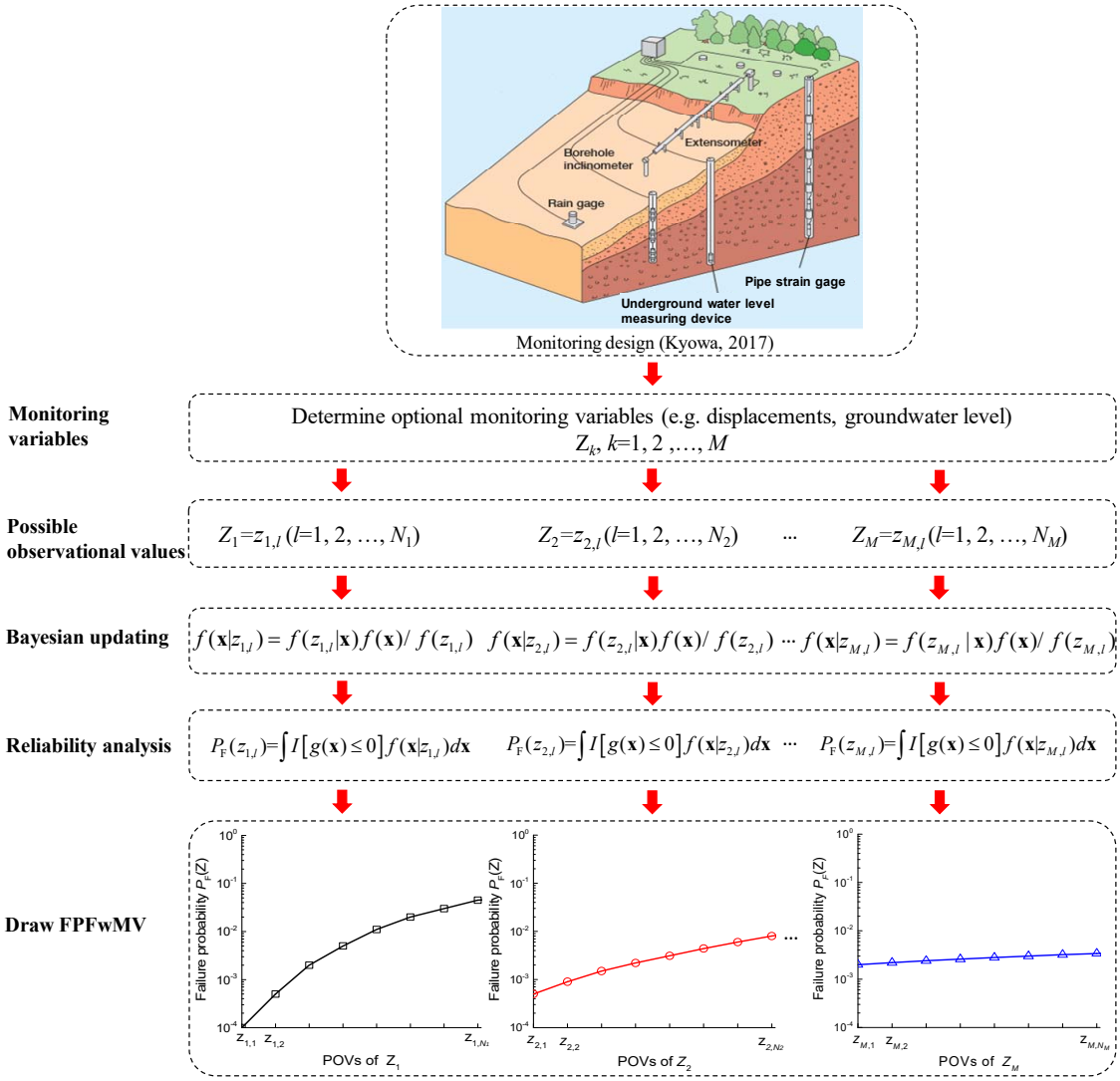

Fig. 1. Reliability sensitivity analysis framework for monitoring variables

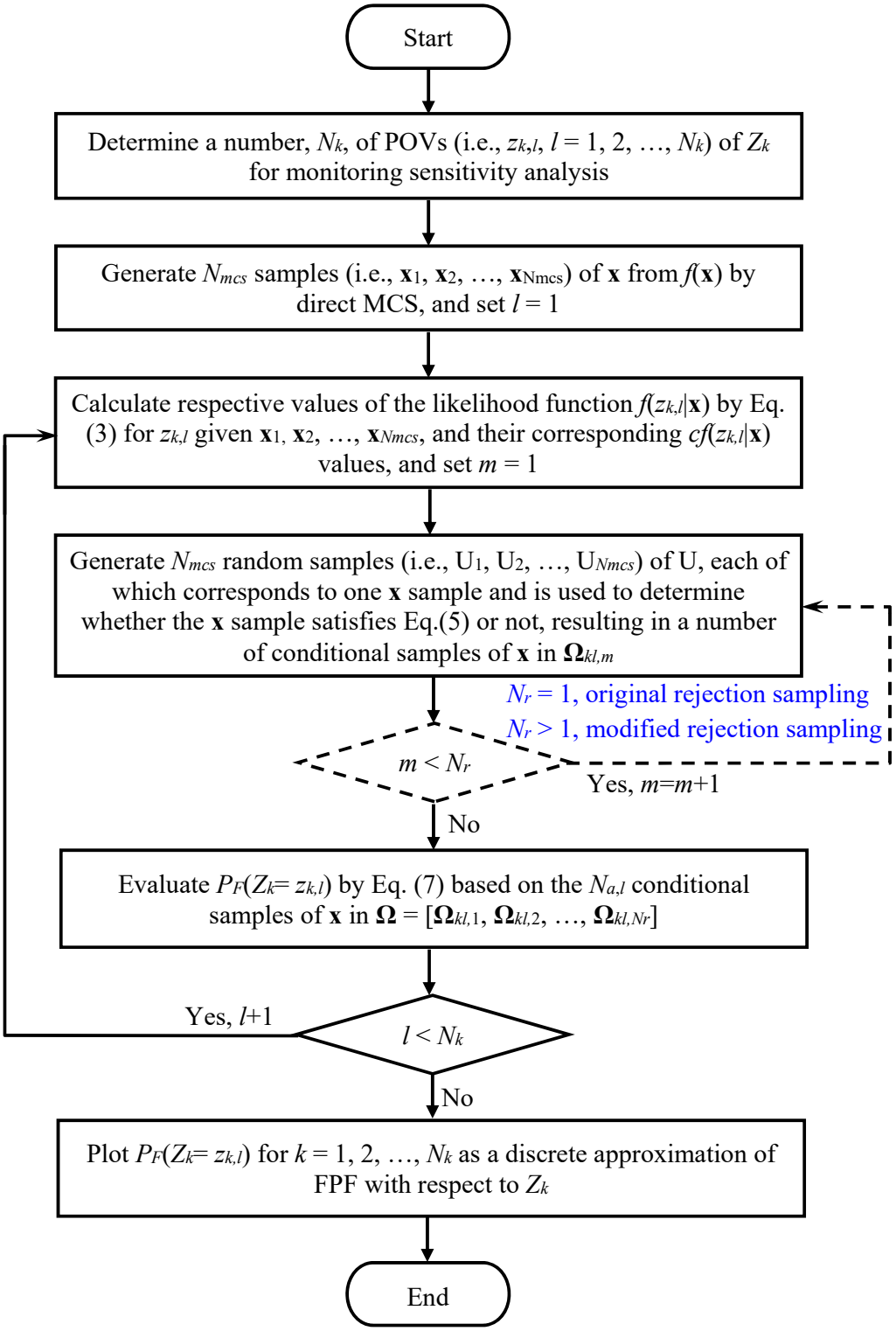

Fig. 2. Implementation procedure of the proposed sample-based strategy for evaluating FPFwMV

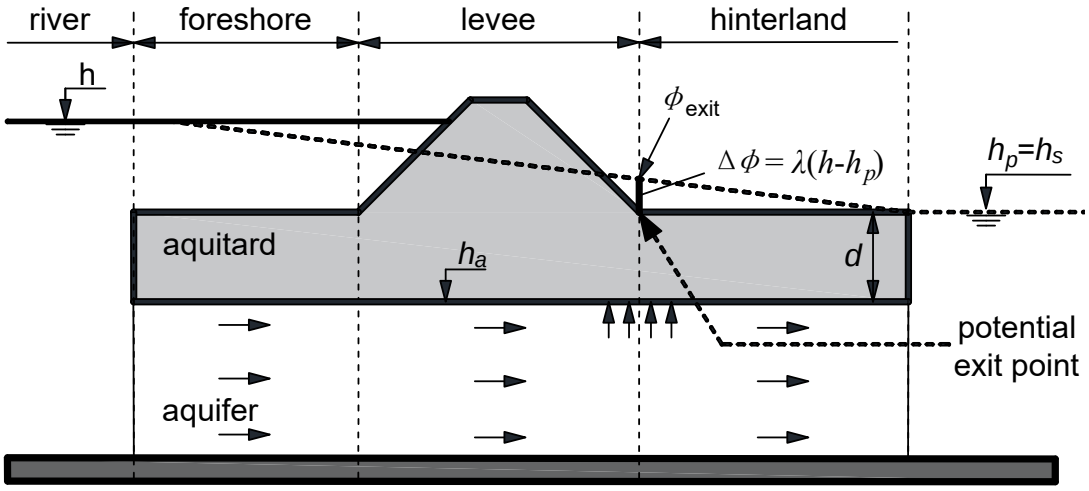

Fig. 3. The levee head monitoring example (after Schweckendiek and Vrouwenvelder 2013)

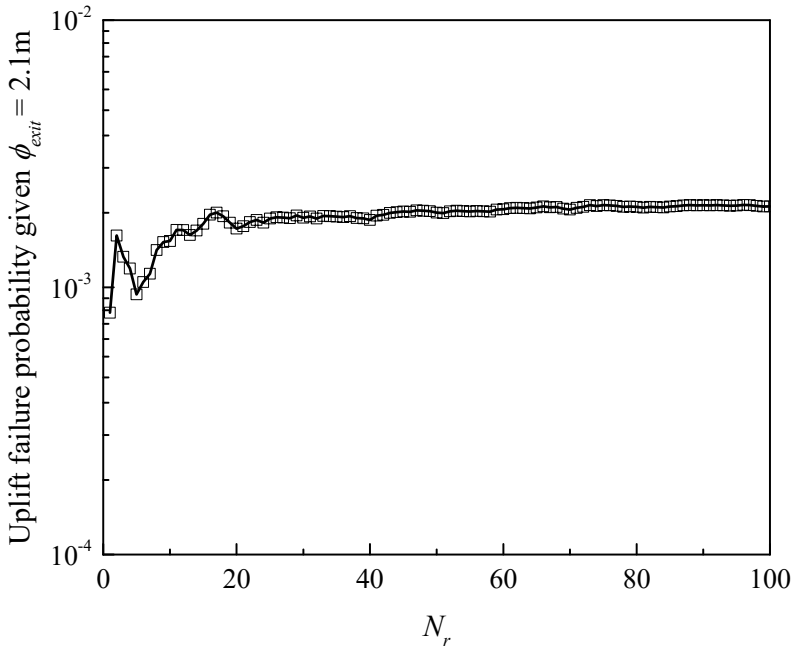

Fig. 4. Variation of the uplift failure probability given ϕ_{exit} = 2.1 m with the increase of N_r

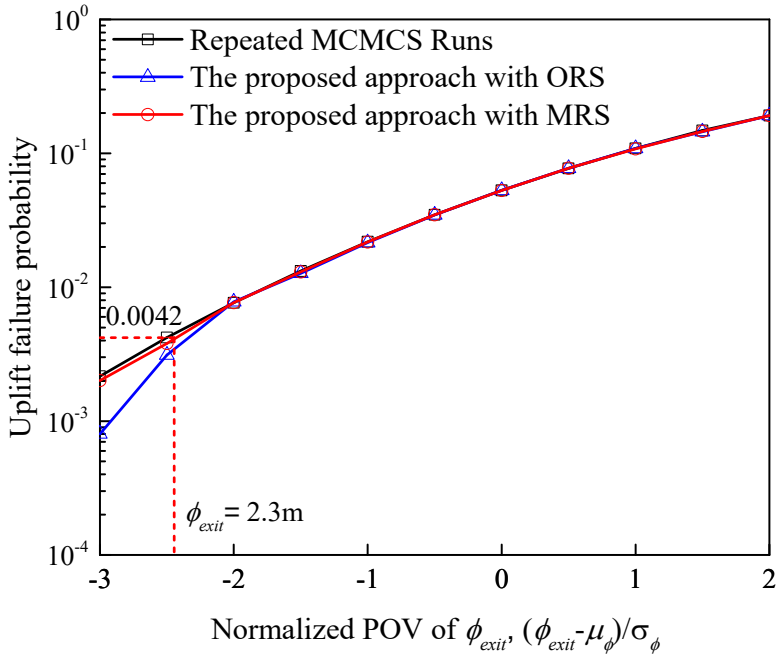

Fig. 5. Comparison of uplift failure probability functions obtained by different methods

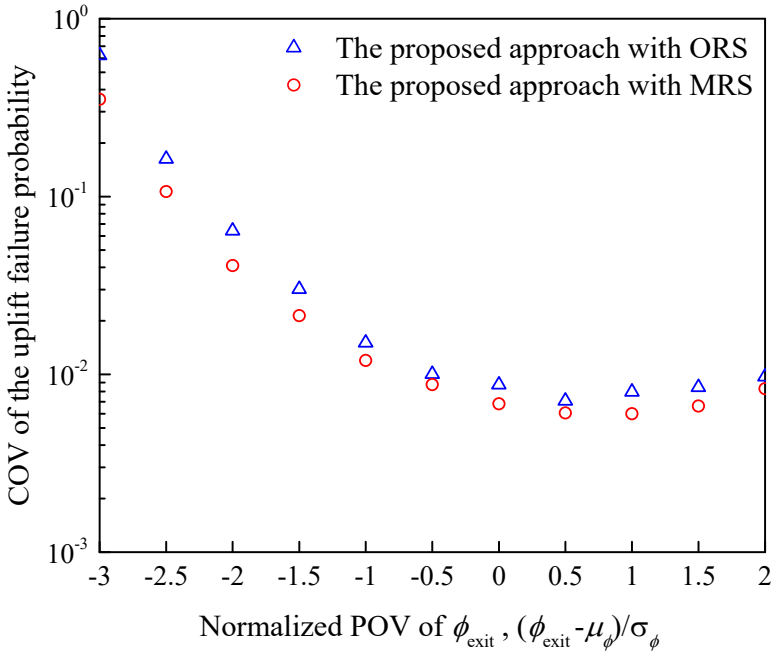

Fig. 6. Coefficients of variation of uplift failure probabilities calculated by the proposed approach with ORS and MRS

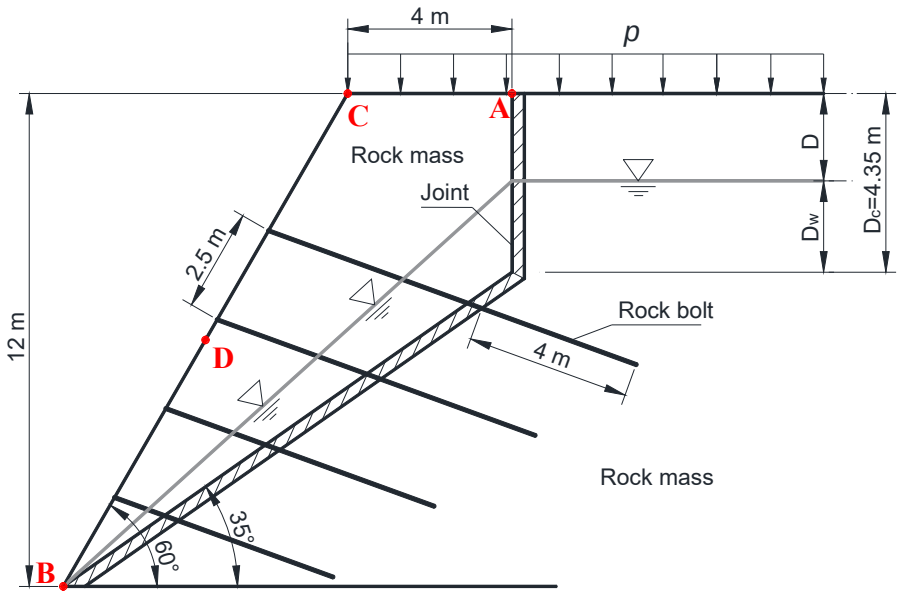

Fig. 7. Illustration of the rock slope example (after Li et al. 2016c)

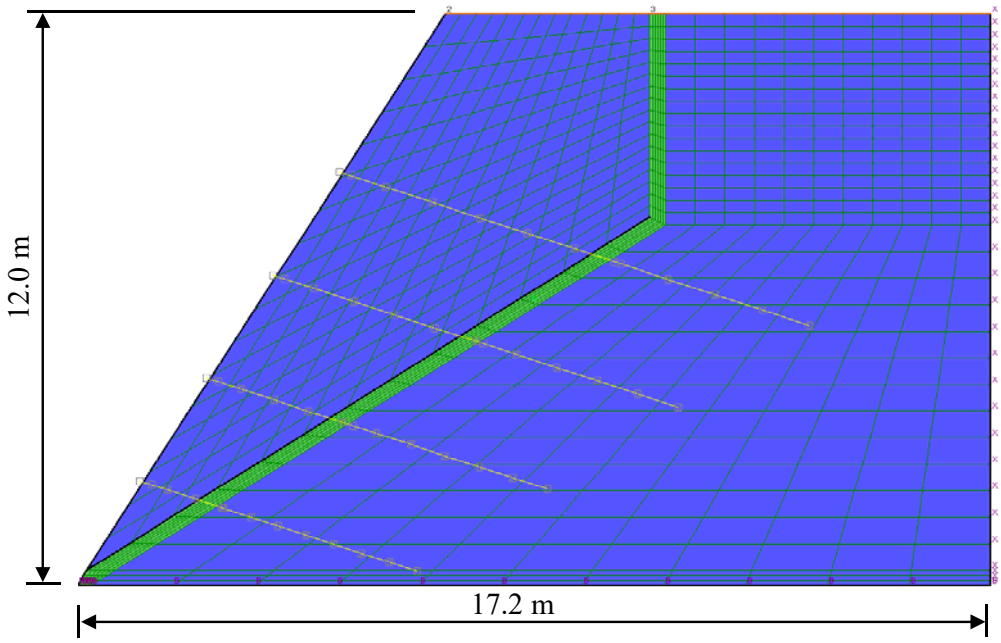

Fig. 8. The finite difference model for the rock slope example in FLAC 7.0

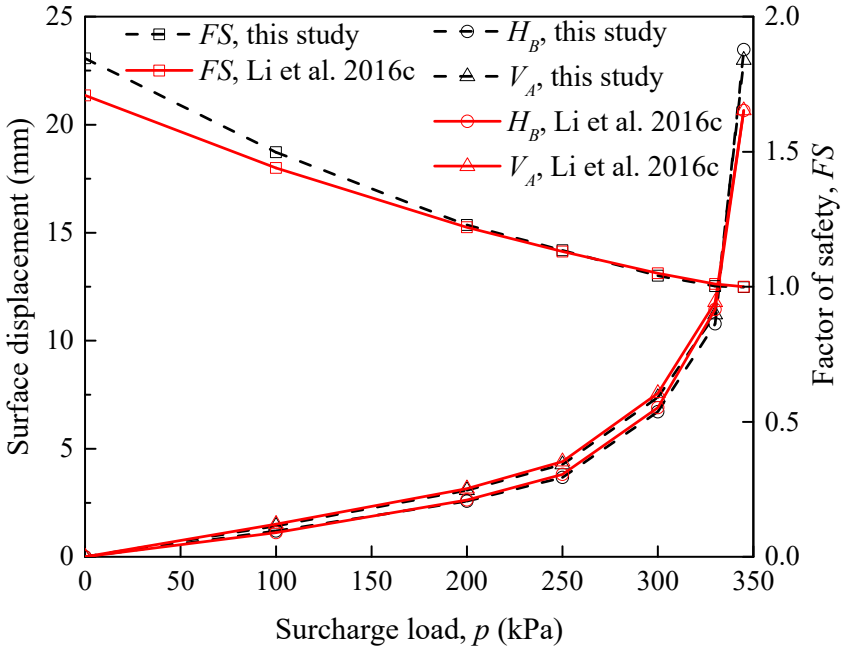

(a) Different surcharge load

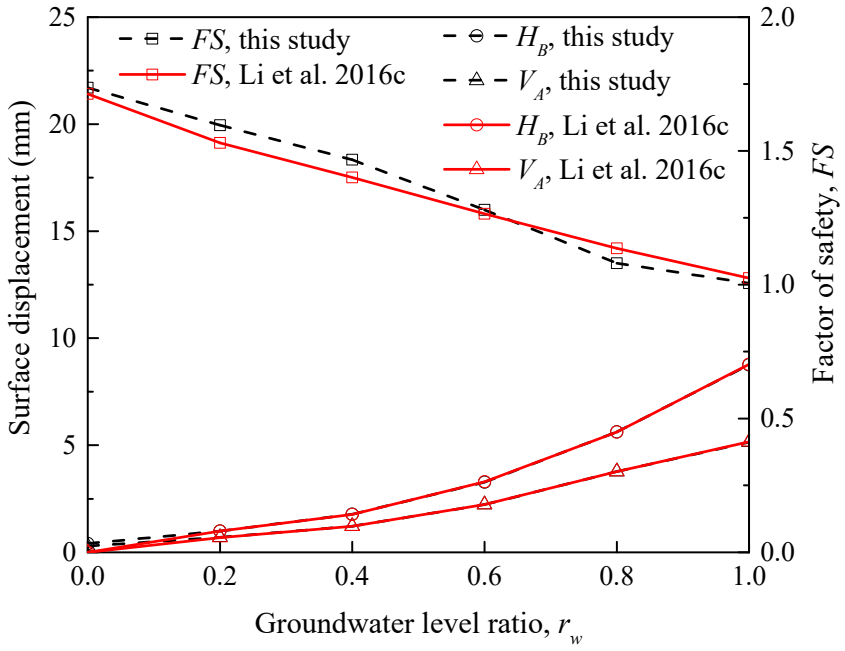

(b) Different groundwater levels

Fig. 9. Factor of safety and surface displacements at points A and B under different surcharge load and groundwater levels

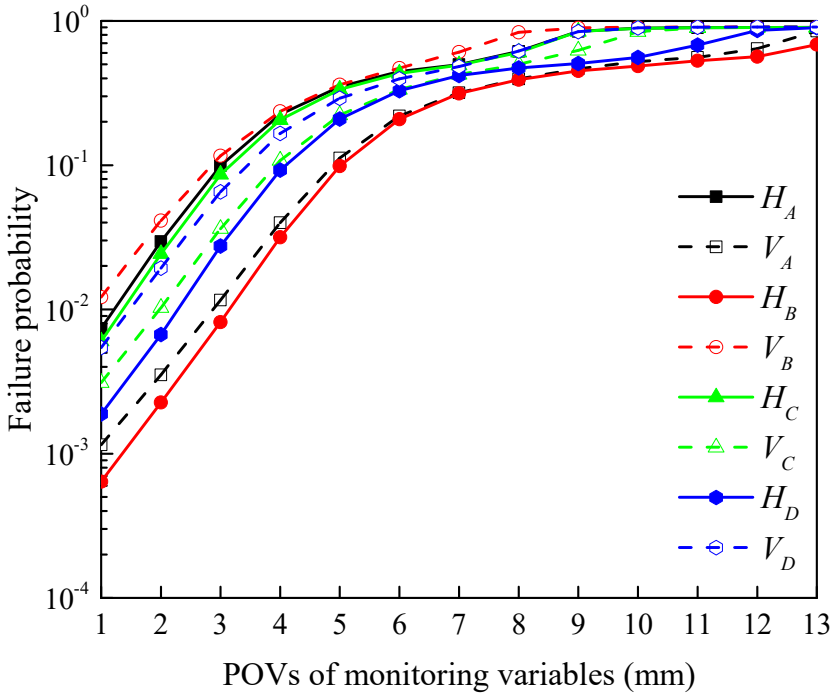

Fig. 10. Failure probability functions with respect to different monitoring variables in the rock slope example